

# Plasma Polymerization of Tetrafluoroethylene

K. NAKAJIMA,\* A. T. BELL, and M. SHEN, *Department of Chemical Engineering, University of California, Berkeley, California 94720*, and M. M. MILLARD, *Western Regional Laboratories, U.S. Department of Agriculture, Albany, California 94710*

## Synopsis

The plasma polymerization of  $C_2F_4$  was carried out in both continuous wave and pulsed rf discharges to establish the effects of reaction conditions on the kinetics of polymer deposition and the polymer structure. ESCA spectra of the polymer show evidence for  $-CF_3$ ,  $-CF_2$ ,  $>CF-$ , and  $-CH_2-$  groups. Under conditions favoring low deposition rates, the dominant functional group is  $-CF_2-$ . At higher deposition rates the concentration of  $-CF_2-$  groups is reduced and a more crosslinked polymer is produced. Both polymer deposition rates and polymer structures were essentially identical when using continuous wave and pulsed rf discharges.

## INTRODUCTION

Plasma-polymerized films of  $C_2F_4$  have potential application as dielectrics,<sup>1,2</sup> corrosion protective coatings,<sup>3</sup> and, as shown most recently, coatings for the orientation of liquid crystals in liquid crystal displays.<sup>4</sup> It is therefore of interest to determine the structure of the films and the effect of deposition conditions on the structure. Several recent studies<sup>5,6</sup> have shown that ESCA can be used to provide information concerning the types of carbon atoms present near the surface of fluorocarbon polymers. Applications of this technique to the study plasma-polymerized fluorocarbons have also been reported.<sup>3,7-10</sup> The present study was undertaken to investigate the effects of reaction conditions upon the polymerization rate of  $C_2F_4$  and the structures of the polymer formed. Experiments were conducted using both continuous wave (cw) and pulsed rf discharges.

## EXPERIMENTAL

Polymerization was carried out in a discharge sustained between two disk electrodes contained within a glass bell jar. Details concerning this reactor have been presented previously.<sup>11</sup> Power for the discharge was supplied at 13.56 MHz by one of two generators. For cw work an IPC Model PM 104B generator was used, while for work with pulsed discharges a Tegal 100-W generator was used. Tetrafluoroethylene containing 2% of limonene ( $C_{10}H_{16}$ ), a polymerization inhibitor, was obtained from PCR, Inc., and used directly without purification. Polymer deposition rates were measured by weighing the amount of polymer deposited on a glass slide in a fixed period of time. For the characterization of polymer structure by ESCA, the polymer was deposited on thin  $1/4$ -in. glass disks.

\* Permanent Address: Sony Corporation, P.O. Box 10, Tokyo, A.P., Tokyo, 149 Japan.

ESCA spectra were recorded on a Dupont 650 spectrometer. To avoid significant x-ray damage of the polymer, only eight scans were accumulated for each sample. The C(1s) portion of each spectrum was deconvoluted into six lines using a nonlinear least-squares fitting routine.<sup>12</sup> Good fits between the predicted and experimental spectra were obtained assuming Lorentzian line shapes with a leading constant tail. The full width at half-maximum of each line was set at 2 eV.

Atomic ratios of fluorine to carbon and oxygen to carbon were evaluated from separate ESCA spectra. A fresh sample was used for each determination, and a single scan was taken of each element. Ratios of the integrated line intensities were corrected for differences in atomic sensitivity by dividing by the ratio of fluorine to carbon or oxygen to carbon sensitivities. The latter ratios were established as 5.6 and 5.3, respectively, from ESCA spectra of samples with known stoichiometries.

## RESULTS AND DISCUSSION

### Rate of C<sub>2</sub>F<sub>4</sub> Polymerization

Figure 1 illustrates the effects of power on the polymer deposition rate. For very low monomer flow rates the deposition rate declines with increasing power, while at high flow rates the deposition rate increases. The observed differences in the effect of power at high and low flow rates can be interpreted in terms of the following reaction network:

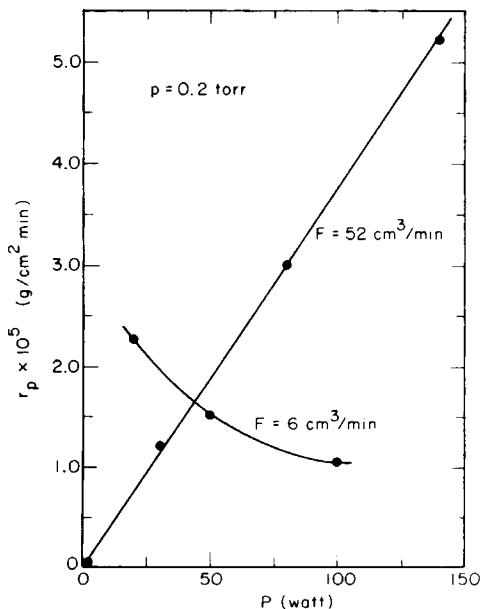
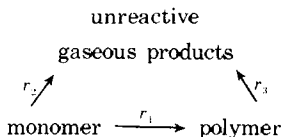


Fig. 1. Effect of power on rate of polymer deposition.

Reaction 1 represents the conversion of monomer  $C_2F_4$  to polymer. This process may be accompanied by the simultaneous conversion of a part of the monomer to unreactive gaseous products, such as saturated fluorocarbons,<sup>13</sup> via reaction 2. Similar products may also be produced by partial decomposition of the deposited polymer through reaction 3. Evidence supporting the proposed network of reactions has recently been presented by Poll et al.<sup>14</sup> and Yasuda et al.<sup>15</sup> Clark and Dilks<sup>16</sup> and Smolinsky and Vasile<sup>13</sup> have noted the ability of a discharge to bring about the decomposition of fluorocarbon polymers.

At low monomer flow rates the deposition of polymer in a discharge is usually limited by the supply of monomer, essentially all of the monomer being converted to either polymer or stable gaseous products.<sup>17</sup> Under these conditions, increasing power would not significantly increase the rate of reaction 1 but would enhance the destruction of the deposited polymer via reaction 3. The net result would be a decline in the rate of polymer deposition with increasing power. By contrast, at high monomer flow rates only a fraction of the monomer is converted to polymer and the deposition rate is normally controlled by the rate of formation of polymer precursors. In this case increasing the discharge power is expected to increase the rate of polymerization. While the rate of polymer destruction is also expected to increase with power, the sensitivity of this reaction to power is apparently not as great as that of the polymerization process, and in the presence of an adequate supply of monomer the net rate of polymer deposition increases with the discharge power.

The effects of pressure on deposition rate are shown in Figures 2 and 3. At 10 W increasing pressure causes the deposition rate to pass through a maximum, while at 50 W only a monotonic increase in deposition rate is found over the same

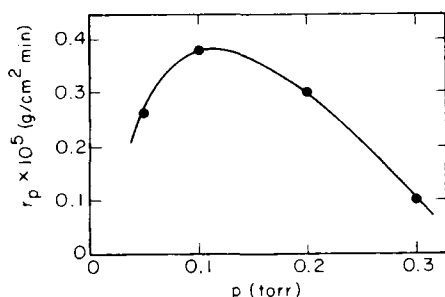


Fig. 2. Effect of pressure on rate of polymer deposition;  $P = 10$  W,  $F = 6$  cm<sup>3</sup>/min.

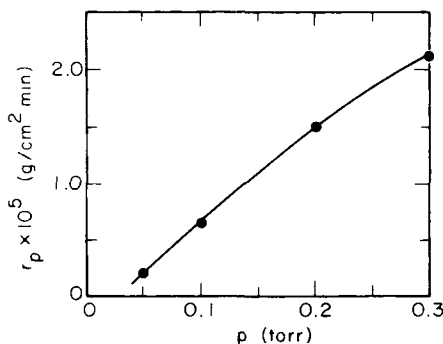


Fig. 3. Effect of pressure on rate of polymer deposition;  $P = 50$  W,  $F = 6$  cm<sup>3</sup>/min.

pressure range. These differences are undoubtedly associated with the complex fashion in which pressure affects deposition rate. In addition to increasing monomer concentration, an increase in gas pressure will reduce both the electron temperature and electron density.<sup>18</sup> The latter effects contribute to a decline in the rate of initiation of polymerization while the former contributes to an increase in the rates of initiation and propagation.<sup>19</sup> Thus, it is possible under certain conditions for an increase in pressure to cause an increase in deposition rate, while under other conditions it is possible for an increase in pressure to cause a decrease in deposition rate.

The effect of  $C_2F_4$  flow rate on the deposition rate is shown in Figure 4. At low flow rates the deposition rate increases with flow rate, but at higher flow rates the deposition rate passes through a maximum and then decreases. Similar effects have been observed for many monomers and can be explained in the following manner.<sup>17</sup> At low flow rates the deposition rate is controlled by the supply of fresh monomer since the monomer residence time is sufficiently high for most of the monomer to be polymerized. As the flow rate is increased to higher levels, the residence time decreases to a point at which the concentration of precursors to polymerization (e.g., free radicals) is no longer high enough to maintain rapid polymerization.

Two sets of experiments were conducted using a pulsed rf discharge. The pulse duration is designated by  $t_{on}$  and the period between pulses by  $t_{off}$ . The ratio  $t_{off}/t_{on}$  is defined as  $r$ , and the average power  $\langle P \rangle$  is given by

$$\langle P \rangle = P_p / (1 + r) \quad (1)$$

where  $P_p$  is the peak power and  $(1 + r)^{-1}$  is the duty cycle.

Figure 5 illustrates the effect of duty cycle on deposition rate. These experiments were carried out using a constant cycle time of  $t_{on} + t_{off} = 2$  msec. The linear relation between deposition rate and duty cycle suggests that all one is observing is the proportionality of the rate to the average power, similar to the trend shown in Figure 1.

To study the influence of pulse duration,  $r$  was set equal to 1, and  $t_{on}$  was varied from 0.2 to 2.0 msec. Figure 6 shows that the deposition rate is insensitive to  $t_{on}$ . These data suggest that the plasma rises to a steady state and then quenches from this state in times small compared to the pulse width.

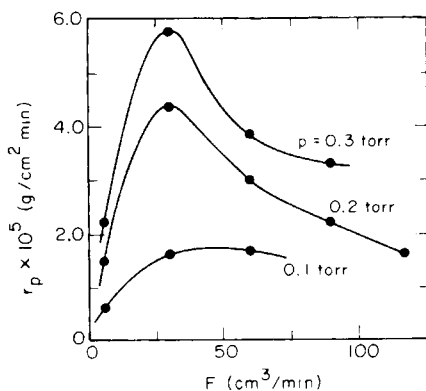


Fig. 4. Effect of flow rate on rate of polymer deposition;  $P = 50$  W.

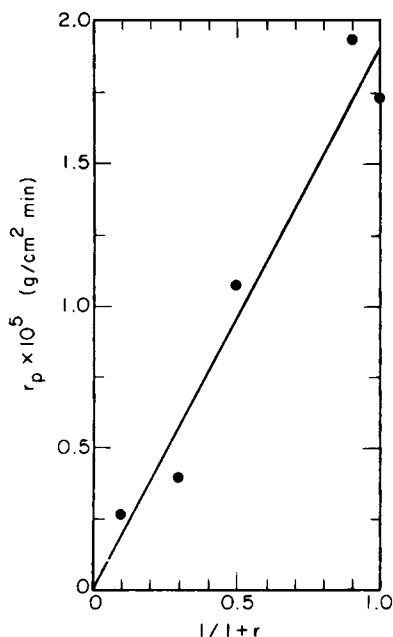


Fig. 5. Effect of duty cycle on the rate of polymer deposition;  $P_p = 80$  W,  $F = 145$  cm<sup>3</sup>/min,  $p = 0.3$  Torr.

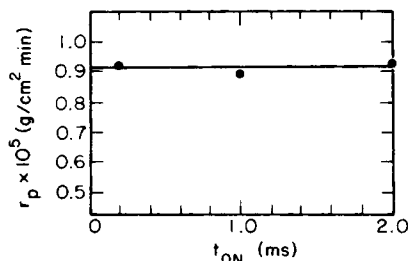


Fig. 6. Effect of pulse duration on the rate of polymer deposition;  $\langle P \rangle = 20$  W,  $F = 60$  cm<sup>3</sup>/min,  $p = 0.2$  Torr,  $r = 1.0$ .

### Characterization of Plasma-Polymerized C<sub>2</sub>F<sub>4</sub>

A representative ESCA spectrum of the C(1s) region is shown in Figure 7. Spectra such as this were deconvoluted into six separate peaks. Table I lists the average binding energy associated with each peak and the standard deviation from the average value. To compensate for sample charging, the binding energy of the highest energy peak was set to 293.8 eV, the energy characteristic of —CF<sub>3</sub> groups. This selection was based upon the observation that the position of —CF<sub>3</sub> peaks is weakly affected by nearest neighbor groups, in contrast to other fluorine-containing groups present in the polymer.

Assignments for the six ESCA peaks are given in Table I. The bond structures shown are based upon ESCA characterizations of PTFE, PTFE/PE copolymers, and PHFP (polyhexafluoropropene) reported by Clark<sup>6</sup> and upon ESCA spectra of low molecular weight fluorocarbons reported by Davis.<sup>20</sup> It is apparent that the peaks appearing at 293.8 and 291.5 eV can unambiguously be assigned to —CF<sub>3</sub> and —CF<sub>2</sub>— groups, respectively. The two bands at 289.5 and 288.2 eV

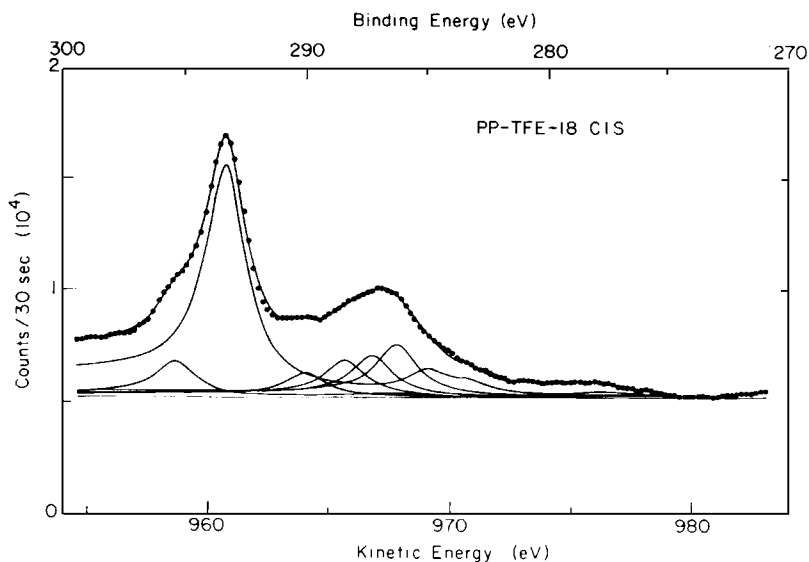


Fig. 7. Representative C(1s) ESCA spectrum of plasma-polymerized  $C_2F_4$ .

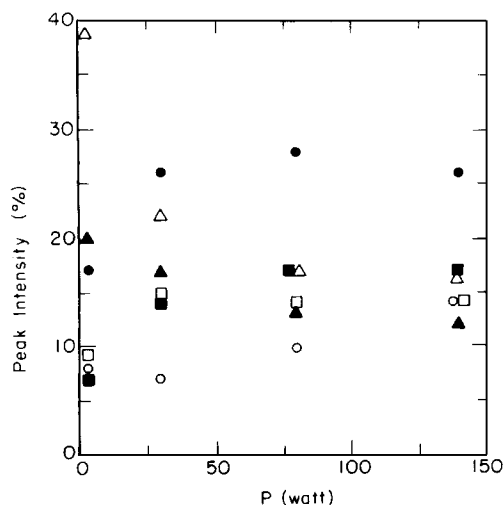


Fig. 8. Effect of power on distribution of C(1s) ESCA peak intensities:  $F = 52 \text{ cm}^3/\text{min}$ ,  $p = 0.2 \text{ Torr}$ .

can be assigned to either  $>CF-$  or  $-CFH-$  groups. A clear-cut distinction between these two groups is not possible inasmuch as it is conceivable that the polymer films prepared contained hydrogen derived from a cracking of the limonene present in the monomer. Since both structures contain only one atom of fluorine per carbon atom, we have designated the peak at 289.5 eV as  $>CF-(II)$ . The remaining two peaks appearing at 286.9 and 285.5 eV are the most difficult to assign. Comparison of the positions of these peaks with those for polymers of known structure suggests that both peaks are due to  $-CH_2-$  groups. The peak appearing at 286.9 eV is most likely associated with  $-CH_2-$  groups adjacent to fluorocarbon groups such as  $-CF_2-$  or  $-CF_3$ . The re-

maining peak, characterized by a binding energy of 285.5 eV, is best assigned to short chains of  $-\text{CH}_2-$  groups. As will be seen, this structure normally accounts for less than 10% of the carbon present in the polymer.

The effects of reaction conditions on the polymer surface structure observed by ESCA are shown in Figures 8 through 14. In each of these figures the relative peak intensity is plotted versus the variable studied.

Figure 8 illustrates the distribution of carbon atom types as a function of discharge power. As the power is increased, a marked decline occurs in the relative intensities of  $-\text{CF}_3$  and  $-\text{CF}_2-$  groups, with corresponding increases in the intensities of  $>\text{CF}-$  and  $-\text{CH}_2-$ (II) groups. Consistent with these trends, the F/C ratio decreases with increasing power as shown in Figure 9. Also shown in Figure 9 is the O/C ratio. The O/C ratio increases with power but is significantly smaller than the F/C ratio at all power levels.

The effects of pressure, shown in Figures 10 and 11, are different, depending upon the power level. At 10 watts, increasing pressure causes an increase in the intensity of  $-\text{CF}_2-$  peaks. The intensities of the  $-\text{CF}_3$  and  $-\text{CH}_2-$ (II) peaks appear to pass through a maximum at about 0.1 torr, the same pressure at which the deposition rate is a maximum. The remaining peaks show either a slightly declining or a nearly constant intensity level. When the power is raised to 50 watts, little if any changes in peak intensity distribution are observed with increasing pressure. Comparing the intensity distributions in Figures 10 and 11

TABLE I  
Assignment of ESCA Peaks

B.E., <sup>a</sup> eV	Bond structure	Symbol <sup>b</sup>	References structures	B.E., eV	Reference
295.5 ± 0.3	$-\text{CH}_2-$ (I)	○	$\{ \text{C}^* \text{H}_2 \text{CH}_2 \}_n$	285.0	6
			$\text{C}^* \text{H}_2 = \text{CHF}$	285.2	20
			$\text{C}^* \text{H}_3 \text{CH}_2 \text{F}$	285.3	20
			$\text{C}^* \text{H}_2 = \text{CF}_2$	285.5	20
			$\text{CF}_3 \text{CH} = \text{C}^* \text{H}_2$	285.7	20
			$\{ \text{CFHC}^* \text{H}_2 \}_n$	285.9	6
286.9 ± 0.1	$-\text{CH}_2-$ (II)	●	$\{ \text{C}^* \text{H}_2 \text{CF}_2 \}_n$	286.6	6
288.2 ± 0.2	$>\text{CF}-$ (I)	□	$\{ \text{C}^* \text{FHCH}_2 \}_n$	288.0	6
			$\text{C}_6^* \text{F}_6$	288.1	20
289.5 ± 0.2	$>\text{CF}-$ (II)	■	$\{ \text{CFHC}^* \text{FH} \}_n$	288.4	6
			$\text{CF}_3 \text{C}^* \text{F} = \text{CF}_2$	288.8	20
			$\text{CF}_3 \text{C}^* \text{F} = \text{CFCF}_3$	289.1	20
			$\{ \text{C}^* \text{FHCF}_2 \}_n$	289.3	6
			$\{ \text{C}^* \text{F}(\text{CF}_3) \text{CF} \}_n$	289.8	6
291.5 ± 0.1	$-\text{CF}_2-$	△	$\text{CF}_3 \text{CF} = \text{C}^* \text{F}_2$	291.1	20
			$\{ \text{C}^* \text{F}_2 \text{CFH} \}_n$	291.6	6
			$\{ \text{CF}(\text{CF}_3) \text{C}^* \text{F}_2 \}_n$	291.8	6
			$\text{CF}_3 \text{C}^* \text{F}_2 \text{CF}_3$	291.9	20
			$\{ \text{CF}_2 \text{CF}_2 \}_n$	292.2	6
			$\{ \text{CF}(\text{C}^* \text{F}_3) \text{CF}_2 \}_n$	293.7	6
293.8 ± 0.0	$-\text{CF}_3$	▲	$\text{C}^* \text{F}_3 \text{CF} = \text{CF}_2$	293.7	20
			$\text{C}^* \text{F}_3 \text{CF} = \text{CFCF}_3$	293.8	20
			$\text{C}^* \text{F}_3 \text{CF}_2 \text{CF}_3$	293.9	20
			$\text{C}^* \text{F}_3 \text{CF}_3$	294.0	20
			$\{ \text{C}(\text{C}^* \text{F}_3) = \text{C}(\text{CF}_3) \}_n$	294.1	6

<sup>a</sup> B.E. = Binding energy.

<sup>b</sup> Symbols are those used in Figures 8 and 10–14.

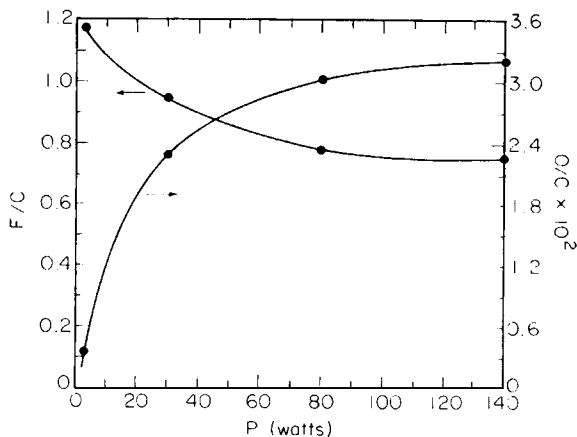


Fig. 9. Effect of power on F/C and O/C ratios:  $F = 52 \text{ cm}^3/\text{min}$ ,  $p = 0.2 \text{ Torr}$ .

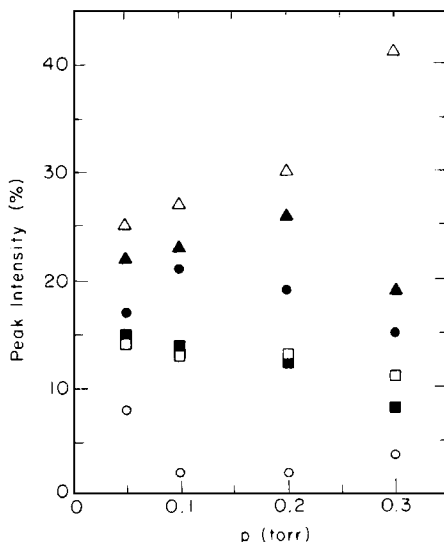


Fig. 10. Effect of pressure on distribution of C(1s) ESCA peak intensities;  $P = 10 \text{ W}$ ,  $F = 6 \text{ cm}^3/\text{min}$ .

it is apparent that the concentrations of  $-\text{CF}_2-$  and  $-\text{CF}_3$  groups tend to be less in the polymer films deposited at higher power.

Changes in polymer structure produced by increasing  $\text{C}_2\text{F}_4$  flow rate are illustrated in Figure 12. It is observed that the intensities of  $-\text{CF}_2-$  and  $-\text{CF}_3$  pass through a minimum while intensities of  $-\text{CF}-$  and  $-\text{CH}_2-$ (I) peaks pass through a maximum. Quite interestingly, the flow rate at which the maxima and minima occur is the same as that for the maximum in deposition rate shown in Figure 4. Finally, we note that the intensity of the  $-\text{CH}_2-$ (II) peak increases monotonically with flow rate.

The characteristics of polymers produced with a pulsed discharge are shown in Figures 13 and 14. The first of these figures illustrates the effects of increasing duty cycle for a constant value of  $t_{\text{on}} + t_{\text{off}} = 2 \text{ msec}$ . There is a very noticeable decline in the relative intensity of the  $-\text{CF}_2-$  peak, with corresponding increases



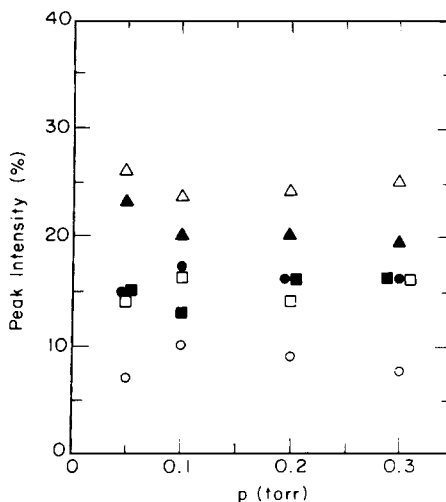


Fig. 11. Effect of pressure on the distribution of C(1s) ESCA peak intensities;  $P = 50$  W,  $F = 6$   $\text{cm}^3/\text{min}$ .

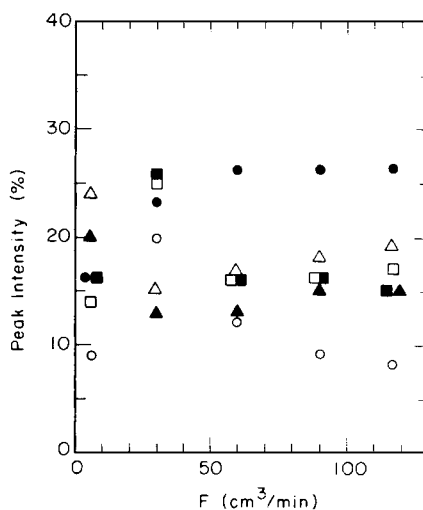


Fig. 12. Effect of flow rate on distribution of C(1s) ESCA peak intensities;  $P = 50$  W,  $p = 0.2$  Torr.

in the intensities of all other peaks as the duty cycle increases. It should be recalled here that as the duty cycle increases, the average power increases proportionately. Thus, the effects of increasing duty cycle are thought to be largely attributable to increasing power. This conclusion is supported by Figure 14, which shows virtually no change in the relative peak intensity distribution as pulse duration is increased from 0.2 to 2.0 msec at a constant duty cycle of 0.5.

The results presented in Figures 8 through 14 indicate that all three fluorine-containing groups (viz.,  $-\text{CF}_3$ ,  $-\text{CF}_2-$ , and  $>\text{CF}$ ) are present with roughly equivalent frequency in the polymer films produced from  $\text{C}_2\text{F}_4$ . This distribution of functional groups is consistent with the general view that plasma-

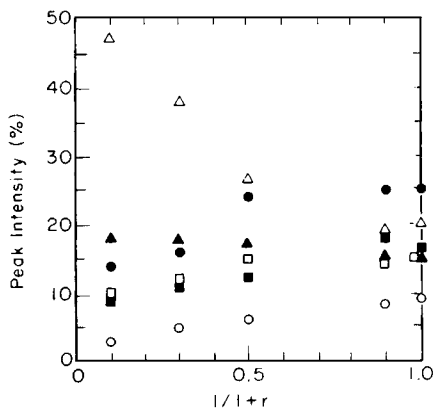


Fig. 13. Effect of duty cycle on distribution of C(1s) ESCA peak intensities:  $P_p = 80$  W,  $F = 145$  cm<sup>3</sup>/min,  $p = 0.3$  Torr.

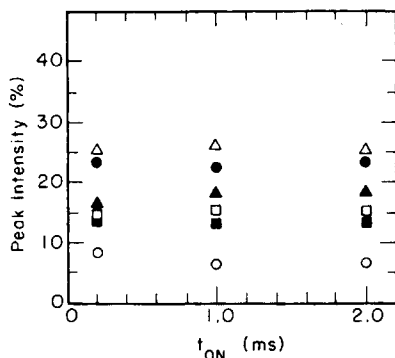


Fig. 14. Effect of pulse duration on distribution of C(1s) ESCA peak intensities;  $\langle P \rangle = 20$  W,  $p = 0.2$  Torr,  $F = 60$  cm<sup>3</sup>/min,  $r = 1.0$ .

deposited polymers are characterized by an irregular network structure. The  $-\text{CF}_2-$  groups comprise the chains of the network which are terminated by  $-\text{CF}_3$  groups. Branch points and crosslinks are represented by  $>\text{CF}-$  groups. The extent of branching and crosslinking in the polymer can be judged from the relative concentrations of  $-\text{CF}_2-$  and  $>\text{CF}-$  groups. It is apparent that films produced at very low deposition rates, corresponding to low power, low monomer flow rate, and high pressure, contain significantly higher concentrations of  $-\text{CF}_2-$  groups than films deposited very rapidly. This suggests that slow deposition conditions favor chain growth over crosslinking. The latter process very likely occurs after the chains are first formed and results from either chain disruption or fluorine atom abstraction by species emanating from the plasma.

Two observations support such a view of the polymer growth process. The first is that PTFE can be formed by allowing  $\text{CF}_3\cdot$  radicals produced in a discharge and then cryogenically trapped to react with condensed  $\text{C}_2\text{F}_4$  monomer.<sup>21</sup> A similar process is expected to occur on the surface of a polymer film being deposited in a plasma. The second observation is that PTFE will lose fluorine atoms when exposed to the action of an inert gas discharge.<sup>13,15,16</sup> ESCA spectra of the treated PTFE surface show a decline in the concentration of  $-\text{CF}_2-$  groups, a rise in the concentration of  $>\text{CF}-$  groups, and a decline in the F/C ratio of the polymer.

The fluorine-to-carbon content of the polymers produced in this work also deserves comment. Surveying the results of many samples it is observed that the F/C ratio of the polymer ranges between 1.43 and 0.75 and is thus significantly lower than 2.0, the ratio in the monomer. The low values of F/C are consistent with the existence of a highly crosslinked polymer structure. However, the occurrence of significant cases in which the F/C is well below unity is surprising. One explanation might be the presence of large concentrations of quarternary carbon atoms. Estimations<sup>22</sup> of the binding energy shift for this species places it at 4.3 eV, in close agreement with the feature which we have assigned to  $\text{>CF—(II)}$  in Table I. In view of the close correlation of the relative intensities of the features appearing at 288.2 and 289.5 eV with changes in reaction conditions, we feel that their assignment to two different types of  $\text{>CF—}$  groups is more appropriate. A second explanation for the low F/C ratios might be that the limonene present in small concentration in the  $\text{C}_2\text{F}_4$  is polymerized preferentially. Such an interpretation would be consistent with the observations of large concentrations of  $\text{—CH}_2\text{—}$  groups in Figures 9 and 12, for example. It is believed that the latter explanation is more likely to be the correct one.

The work at the University of California was supported by a grant from the National Science Foundation.

### References

1. H. Pachonik, *Thin Solid Films*, **38**, 171 (1976).
2. J. M. Tibbitt, A. T. Bell, and M. Shen, *J. Macromol. Sci.—Chem.*, **A10**, 519 (1976).
3. D. F. O'Kane and D. W. Rice, *J. Macromol. Sci.—Chem. A*, **10**, 567 (1976).
4. G. J. Sprokel and R. M. Gibson, *J. Electrochem. Soc.*, **124**, 557 (1977).
5. C. R. Ginnard and W. M. Riggs, *Anal. Chem.*, **44**, 1310 (1972).
6. D. T. Clark, in *Structural Studies of Macromolecules by Spectroscopic Methods*, K. J. Ivin, Ed., Wiley, New York, 1976.
7. M. M. Millard, J. J. Windle, and A. F. Pavlath, *J. Appl. Polym. Sci.*, **17**, 2501 (1973).
8. H. R. Anderson, F. M. Fowkes, and F. J. Hielscher, *J. Polym. Sci., Polym. Phys. Ed.*, **14**, 879 (1976).
9. B. D. Washo, *J. Macromol. Sci.—Chem. A*, **10**, 559 (1976).
10. M. M. Millard and A. F. Pavlath, *J. Macromol. Sci.—Chem. A*, **10**, 579 (1976).
11. H. Kobayashi, A. T. Bell, and M. Shen, *J. Appl. Polym. Sci.*, **17**, 885 (1973).
12. C. S. Fadley, Ph.D. Thesis, University of California, UCRL 19535, Berkeley, 1970.
13. M. J. Vasile and G. Smolinsky, submitted to *J. Phys. Chem.*
14. H. U. Poll, M. Arzt, and K. H. Wickleder, *Eur. Polym. J.*, **12**, 505 (1976).
15. H. Yasuda, *J. Macromol. Sci.—Chem. A*, **10**, 383 (1976).
16. D. T. Clark and A. Dilks, in *Characterization of Metal and Polymer Surfaces*, Vol. II, L. H. Lee, Ed., Academic, New York, 1977.
17. J. M. Tibbitt, R. Jensen, A. T. Bell, and M. Shen, *Macromolecules*, **10**, 647 (1977).
18. A. T. Bell, in *Techniques and Applications of Plasma Chemistry*, J. R. Hollahan and A. T. Bell, Eds., Wiley, New York, 1974.
19. A. T. Bell, *J. Macromol. Sci.—Chem. A*, **10**, 369 (1976).
20. D. W. Davis, Ph.D. Thesis, University of California, LBL-1900, Berkeley, 1973.
21. S. V. R. Mastrangelo, *J. Am. Chem. Soc.*, **84**, 1122 (1962).
22. M. Pender, A. T. Bell, and M. Shen, unpublished theoretical determinations of chemical shifts in fluorocarbon polymers.

Received December 23, 1977